Revista de Metalurgia
April-June 2021, 57 (2), e194
ISSN-L: 0034-8570
https://doi.org/10.3989/revmetalm.194

Mechanical and microstructural analysis in the welding of ductile cast iron by TIG procedure, with different filler materials and air cooling

Jorge Martínez Alcón[a], Manuel Pascual Guillamón[b], Lorenzo Solano García[c], Fidel Salas Vicente[b]

[a] PhD student at the Department of Mechanical and Materials Engineering, Polytechnic University of Valencia, 46022 Valencia, Spain

[b] Institute of Materials Technology, Polytechnic University of Valencia, 46022 Valencia, Spain
[c] Department of Mechanical and Materials Engineering, Polytechnic University of Valencia, 46022 Valencia, Spain

(*Corresponding author: jorgemartinezalcon@gmail.com)

Submitted: 14 May 2020; Accepted: 25 February 2021; Available On-line: 30 June 2021

ABSTRACT: The present work analyses the strength and microstuctural variations of ductile cast iron welded by means of the TIG technique, without heat treatment and using different filler materials (pearlitic malleable cast iron, Fe-Ni alloy and bronze and manganese alloy). The specimens for the mechanical and microstructural tests are obtained from each welded coupon with dimensions 100x 100x6 mm. Based on the qualitative analysis of the micrographs and the quantitative analysis of the results of the mechanical tests, which have been carried out in well-differentiated areas of the welded joints (base metal, interface and weld bead), it is concluded that this type of welding and the introduction of new variables such as the heat treatments before and/or after welding are suitable. The mechanical and strength characteristics have been correlated with the microstructures obtained in the plates (specimens) in order to evaluate their advantages and disadvantages, as well as to draw conclusions.

KEYWORDS*:* Base metal; Interface-weld bead; Ductile cast iron; Repair; TIG weldability

Citation/Citar como: Martínez Alcón, J.; Pascual Guillamón, M.; Solano García, L., Salas Vicente, F. (2021). "Mechanical and microstructural analysis in the welding of ductile cast iron by TIG procedure, with different filler materials and air cooling". *Rev. Metal.* 57(2): e194. https://doi.org/10.3989/revmetalm.194

RESUMEN: *Análisis mecánico y microestructural en soldadura de fundición dúctil, mediante procedimiento TIG, con diferentes materiales de aporte y enfriamiento al aire***.** En el presente trabajo se analizan las variaciones resistentes y microestructurales de la fundición dúctil soldada mediante la técnica tungsten inert gas (TIG), sin tratamientos térmicos y utilizando diferentes materiales de aporte (fundición maleable perlítica, aleación Fe-Ni y aleación de bronce y manganeso). A partir de cada cupón soldado de dimensiones 100x100x6 mm, se obtienen las probetas para los ensayos mecánicos y microestructurales. Con el análisis cualitativo de las micrografías y el análisis cuantitativo de los resultados de los ensayos mecánicos, que han sido realizados en zonas bien diferenciadas de las uniones soldadas (metal base, interfase y cordón de soldadura), se concluye la idoneidad de este tipo de soldaduras y de la introducción nuevas variables como los tratamientos térmicos previos y/o posteriores a la soldadura. Se han correlacionando las características mecánicas y resistentes con las microestructuras obtenidas en las placas (probetas) para poder evaluar sus ventajas e inconvenientes, así como elaborar conclusiones.

PALABRAS CLAVE*:* Fundición dúctil nodular; Metal-base-interfase-metal de soldadura; Reparación; Soldabilidad; TIG

ORCID ID: Jorge Martínez Alcón (https://orcid.org/0000-0001-6139-5059); Manuel Pascual Guillamón (https://orcid.org/0000-0003-0216-5119); Lorenzo Solano García (https://orcid.org/0000-0003-0535-314X); Fidel Salas Vicente (https://orcid.org/0000-0003-0834-4425)

1. INTRODUCTION

Ductile cast irons, also known as spheroidal graphite cast irons and to a lesser extent as nodular cast irons UNE-EN 1563 (2019), are alloys of iron (Fe), carbon (C) and silicon (Si), composed of 3-4.3% carbon and 1.3%-3% silicon. (De La Torre *et al.*, 2014).

In the spheroidal cast iron, the graphite takes the form of nodules, thanks to the presence of small proportions of magnesium (Between 0.03-0.06% by weight of magnesium), which is added just at the moment of casting and is retained by the iron; these nodules are distributed uniformly throughout the matrix, eliminating the discontinuities caused by the graphite veins present in the grey cast iron. (Suárez-Sanabria and Fernández-Carrasquilla, 2006).

These alloys provide a wide range of mechanical properties (Wube Dametew, 2015; Marques *et al.*, 2019), defined by their microstructure and their low levels of defects, which are typical of castings. This is due to the high fluidity conferred by the high carbon content and the low melting point (Abboud, 2012; De La Torre *et al.*, 2014; Wube Dametew, 2015). As a result of these characteristics, nodular cast irons are currently the most widely produced cast alloys in the world (Kumar *et al.*, 2017).

The difficulty associated with the welding of cast irons is well known, mainly due to the risk of the appearance of cracks and other defects caused by the contraction phenomena and the formation of fragile microstructures that accompany the fusion welding of this type of material (Askari-Paykani *et al.*, 2014). This circumstance justifies the recommendations to minimise the heat input during the welding process and to carry out pre-heating and/or post-welding heat treatments (Gouveia *et al.*, 2018).

Despite this, it is not always feasible to follow these recommendations. For example, with regard to heat treatments, the size and disposition of the parts to be joined may make them economically or technically non-viable. This is particularly true for the repair of large pieces and for all kinds of on-site repairs, such as those carried out in the shipbuilding industry.

On the other hand, the ease of control of the TIG process with respect to SMAW welding and the possibility of extending the range of filler materials in TIG regarding GMAW process (Wube Dametew, 2015; Bhatnagar and Gupta, 2016), may justify the convenience of performing the welding of cast iron by means of the TIG process, despite its high energy density.

The present work studies the weldability of ductile cast iron by TIG procedure, its choice, despite constituting a more difficult technique to execute, is justified by obtaining cords that are more resistant, more ductile and less sensitive to corrosion than in the rest of the procedures, in addition to the deformation that occurs in the vicinity of the weld bead is less. It has a good surface finish, which can be improved with simple finishing operations, which has a favorable impact on repair and production costs Applies with different filler metals (Chamim *et al.*, 2017) and air cooling, based on the analysis of the microstructural and strength characteristics of the resulting welded joint in each case.

In general, microstructural and strength characteristics are closely related. And, specifically, the properties of ductile cast iron are largely determined by the type of matrix, the presence of defects in the matrix and the size, the shape and the distribution of the graphite nodules (Marques *et al.*, 2019).

It justifies the importance of considering certain variables in the welding process that affect the microstructure of the welded joint, such as the type of filler material. All of this is done with the aim of evaluating the industrial application, for example for cold repairs, of this type of welding as a function of the variation in its characteristics with respect to those of the base metal.

2. COMPOSITION AND MECHANICAL CHARACTERISTICS OF THE CAST IRON AND THE FILLER MATERIALS USED

The base material (Fig. 1) on which the welds have been made is a GJS 400-15 ferritic-pearlitic spheroidal graphite cast iron, which is identified as "GJS 400-15" in Table 1. This table shows the values of the concentration, as a percentage, of different chemical elements for the base material and for each of the filler materials used in this study. These filler materials have been: (Fig. 2) pearlitic malleable cast iron; (b) Fe-Ni alloy; and (c) bronze and manganese alloy, which have been identified in Table 1 as "Malleable", "Fe-Ni" and "Cu-Sn-Mn" respectively.

2.1. GJS400-15 ferritic-pearlitic spheroidal graphite cast iron

The basic material for the experiment was obtained from a commercial cast iron plate of ferritic pearlitic matrix, with a tensile strength of 420 MPa and an elongation of 14%. According to the UNE classification, this material is called "GJS 400-15", where the first value (400) corresponds to the tensile strength in MPa and the second (15) corresponds to the minimum elongation in percent.

In this type of ductile cast iron, the carbon is mainly found in the form of spheroidal graphite (Wube Dametew, 2015; Cárcel-Carrasco *et al.*, 2017) 6 %Ni; and (II. According to UNE-EN 1563 (2019) spheroidal graphite cast irons can be classified into two main groups: ferritic-pearlitic cast irons of spheroidal graphite and ferritic cast irons of spheroidal graphite hardened by solid solution. According to this standard, the base ma-

Table 1. Chemical composition of the base material and filler materials

	C	Mn	S	Ni	Cu	Si	P	Cr	Mo	Mg	Fe
GJS400-15	3.71	0.044	0.007	0.02	0.026	2.8	0.02	0.03	< 0.01	0.032	
Malleable	2.5	0.40	0.01			1.1	0.09				
Fe-Ni	<0.1	0.5-1.5	<0.03	50-61	<1.0	<0.2	<0.03				Rest
Cu-Sn-Mn					88						Rest

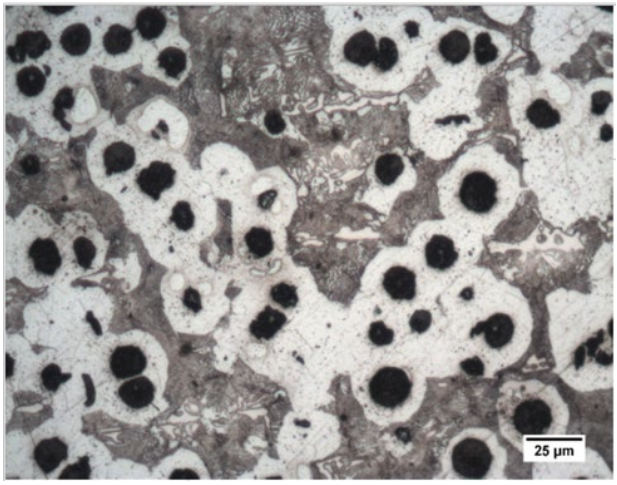

Figure 1. Micrograph of ductile cast iron (base material).

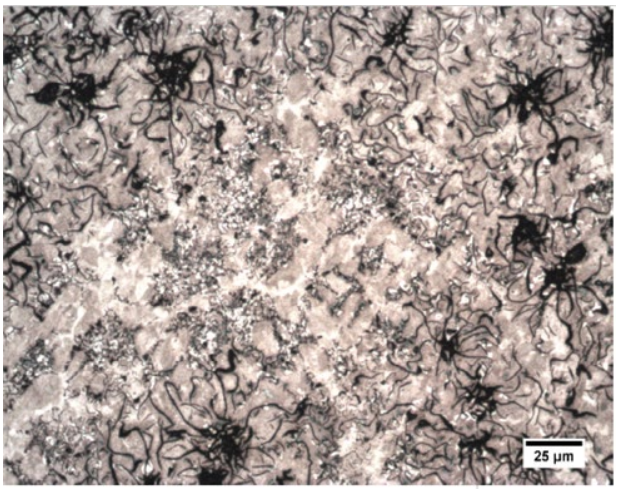

Figure 2. Micrograph of pearlitic malleable cast iron (filler material).

terial used belongs to the first group, which contains ferrite or pearlite, or a combination of them.

2.2. Pearlitic malleable cast iron

Pearlitic malleable cast iron (Fig. 2) is obtained from a white cast iron by a process that starts with slow heating up to 900 ºC and maintaining this temperature in a neutral atmosphere. Subsequently, a slow cooling to approximately 670 ºC is carried out and ends with air cooling.

2.3. Fe-Ni alloy

The Fe-Ni alloy (Fig. 3) used as filler material is of high strength, can be mechanized with cutting tools and has good corrosion resistance (Pascual *et al.*, 2009). It is suitable for cold welding (without heat treatment or preheating of parts) of grey cast irons and malleable cast irons, and also for the joints of these with steels.

2.4. Bronze and manganese alloy

The bronze and manganese alloy (Fig. 4) used as filler material is of high strength, can be machined with cutting tools and has good corrosion resistance. It is obtained through casting processes and is suitable for cold welding of grey cast irons and malleable cast irons, and also for the joints of these with steels. Finally, Table 2 shows the mechanical characteristics of the base material and the filler materials.

3. PREPARATION OF SAMPLES AND WELDING PROCESS

The specimens were obtained from plates of 50x100 mm and 6 mm of thickness, and with a chamfer of 30º in its greater side, that later were welded, according to the regulations, obtaining the welded coupons of dimensions 100x100x6 mm.

All the welds were made using the TIG process, but with three types of electrodes: ER filler rod of

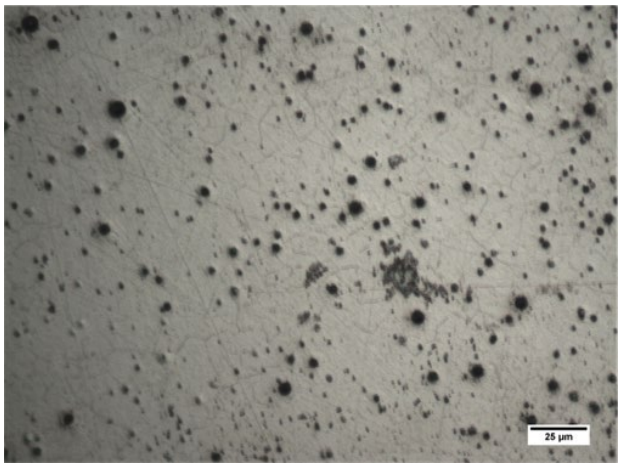

Figure 3. Micrograph of Fe-Ni alloy (filler material).

malleable cast iron; ER (Fe-Ni) commercial filler rod of 2.4 mm diameter; and commercial rod of manganese bronze of 2.4 mm diameter. Welding intensity was maintained between 125 A and 130 A, with a voltage of 14 V, direct polarity and an Argon gas flow rate of 12 litres per minute. In all cases, the weld bead was made in two passes (the first one from the root) and applying the hammering techniques in the filler layer. Both with a circular movement of advance in the horizontal plane and from right to left, angle of inclination of the torch between 70 and 80º according to the advance movement and angle of inclination of the filler rod of about 20º on the horizontal plane. The welds were made in the air, in cold, without heat or mechanical treatments and with air cooling.

Figure 4. Micrograph of the bronze and manganese alloy (filler material).

Considering the difficulty in the welding process presented by cast irons, and in order to avoid cracking due to the stresses generated during the cooling, the welding has been performed in beads of about 30 mm in length and separated from each other by about 30 mm. The hammering is carried out only in the filling phase, when the material cools down, in order to release the residual stresses generated that may cause cracks in the weld (El-Banna, 1999; Cárcel-Carrasco *et al.*, 2016). Another disadvantage is the lack of fluidity of the cast irons in the liquid state, which makes it difficult to drag the material to materialise the joint and favours the appearance of pores (Sellamuthu *et al.*, 2018).

In order to mitigate these disadvantages, the preparation has been carefully carried out, leaving an adequate separation in order to avoid bites and ensure good penetration. In addition, to avoid inclusions, the base material and the filler material of the bare rod were cleaned and deoxidised.

During the welding process, due to the heating of the material, less heat is needed to avoid possible bites on the root of the material (Bhatti *et al.*, 2015). But the current intensity was not reduced, as this could lead to sticker breaks. Instead, the travel speed was increased. After completing each weld, the joints were immediately covered with refractory material for slow cooling (Merchant Samir, 2015).

The next step was to carry out the mechanical and microstructural tests. From each coupon, three specimens of 50 mm length and 20 mm width were obtained, one for the tensile test, other for the micrographic test and another for the hardness test (Ebrahimnia *et al.*, 2012).

4. RESULTS Y DISCUSSION

The final results of each test (tensile test, yield strength, unit elongation and microhardness), shown in Table 3, have been calculated as the average value of a series of five measurements for microhardness.

The tensile tests to determine the mechanical characteristics have been done according to the UNE-EN 10002-1 (2002) for tensile tests at room temperature with a universal testing machine for a maximum force of 10 Tm. The Vickers microhardness (HV) tests have been carried out according to the UNE-EN 876 (1996) with 300 g loads for 10 s with a diamond point at 136º. Three zones were evaluated (Fig. 5) the material adjacent to the weld, the metal-weld interface and the weld zone: a total of nine values. The results are discussed for each of the filler materials used in the

Table 2. Mechanical characteristics of the base material and filler materials

Mechanical characteristics		Spheroidal graphite cast iron	Pearlitic malleable cast iron	Ni-Fe alloy rod	Bronze-Manganese alloy
Tensile strength	MPa	420	325	500	687.25
Yield strength	MPa	340	305	450	305
Elongation	%	14	9	20	9
Elastic modulus	MPa	160000	130000	180000	130000
Brinell hardness		190	235	200	235
Fatigue limit	MPa	170	115	185	115

welds of the ferritic-pearlitic spheroidal graphite cast iron GJS 400-15 and particularly in the areas affected by heat in the weld (Fig. 5).

4.1. Pearlitic malleable cast iron filler material

The pictures in Fig. 6 show the microstructures corresponding to three areas of the welded joint. In the base material zone near the interface (Fig. 5a) the structure consists of graphite nodules in pearlitic matrix almost entirely, with small cementite precipitates, presenting a hardness of 335 HV, normal values for cast irons.

In the interface zone (Fig. 6b), a columnar cementite structure in a pearlitic matrix is observed, a typical white cast iron structure with untransformed ledeburite precipitates. The graphite is spheroidal, smaller than the base material and regularly distributed, and the hardness is 510 HV. Finally, in the weld zone (Fig. 6c), the structure is of nodular graphite close to the interface, which decreases in size and adopts a malleable cast iron structure as it moves away from this zone, the matrix is fine pearlitic with hardness 290 HV. In the tensile tests carried out with standardized specimens, the average joint strength is 370 MPa.

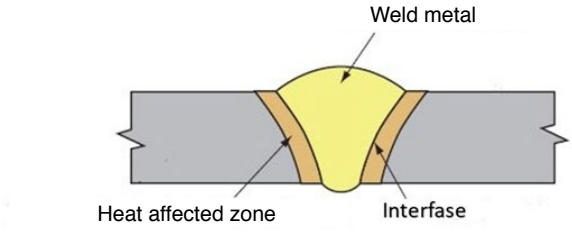

Figure 5 Zones affected by heat in welding.

4.2. Fe-Ni alloy filler material

As in the previous section, the images in Fig. 7 show the microstructures corresponding to three areas of the welded joint. In the base material zone near the interface (Fig. 7a) the structure is made up of graphite nodules, almost entirely in pearlitic matrix, with small cementite precipitates. The elongated white forms correspond to ledeburite, which has a high hardness and fragility. The brown zone corresponds to martensite and the black grains are nodules of dispersed graphite, presenting a hardness of 470 HV, a high value for cast irons. As a consequence, there are an increase in fragility and a decrease in malleability.

In the interface zone (Fig. 7b), a structure similar to that of Fe-Ni cast iron can be seen, which is characterized as being very hard, with graphite nodules. Due to the mixture of the cast iron with the nickel, a structure of traces of columnar cementite in pearlitic matrix with small precipitates of untransformed ledeburite can be observed. The graphite is generally spheroidal, smaller than the base material and regularly distributed. The hardness is 650 HV.

In the weld zone (Fig. 7c), the structure near the interface is of nodular graphite in austenitic matrix, the basic structure of Fe-Ni alloy with some carbides and almost imperceptible dendritic austenitic

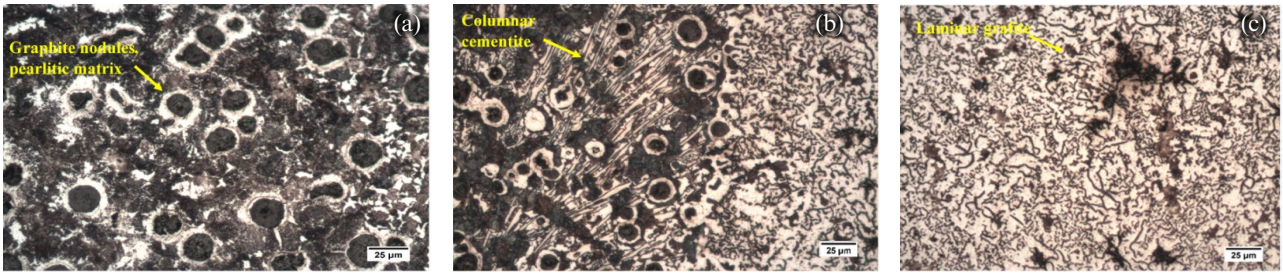

Figure 6 Micrograph of FGE welding with filler rod of commercial malleable cast iron: (a) HAZ (base metal), (b) Interface, and (c) Welding.

Table 3. Mechanical characteristics in different zones of the welded joint: HAZ (heat affected zone), bead and interface

Mechanical characteristics		Pearlitic malleable cast iron	Ni-Fe alloy	Bronze-manganese alloy
Tensile strength	(MPa)	370 ± 18	353 ± 18	147 ± 18
Yield strength	(MPa)	330 ± 18	320 ± 15	138 ± 15
Elongation	(%)	9	10	4
Hardness (HAZ)	(HV)	335	470	239
Hardness (bead)	(HV)	290	301	382
Hardness (interface)	(HV)	510	650	608

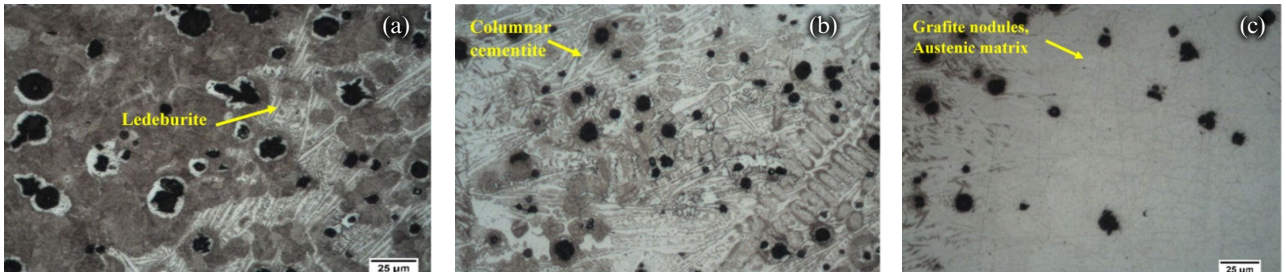

Figure 7. Micrographs of FGE welding with commercial filler rod ER Ni-Fe at 60% Ni without prior heat treatment: (a) HAZ (base metal), (b) Interface, and (c) Welding.

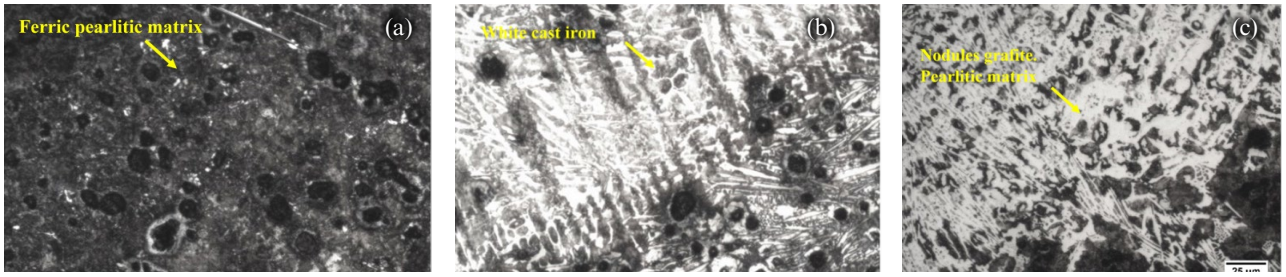

Figure 8. Welding of nodular cast iron with filler rod of manganese bronze: (a) HAZ (base metal), (b) Interface, and (c) Welding.

grain. The hardness is 301 HV and the average tensile strength in the welded joint is 353 MPa, somewhat lower than the welded specimen with pearlite malleable cast iron.

4.3. Filler material of bronze and manganese alloy

In the area of the base material near the interface (Fig. 8a), a ferric-pearlitic structure can be seen, where the matrix is pearlitic with nodular graphite and with traces of ferrite around the nodules. This type of structure has a low hardness of 239 HV.

In the interface area (Fig. 8b) a white cast iron is visible, where nodular graphite is also present, uniformly distributed and of smaller size than in the structure that makes up the base metal. Untransformed ledeburite into an austenitic matrix can be observed. As a consequence, the hardness is increased in this area up to 608 HV. In the weld zone (Fig. 8c) there is a structure similar to that of the interface of white cast iron in an austenitic matrix, with small traces of ledeburite that has not been transformed and with combined graphite forming the white cast iron (pearlite and cementite). This structure makes it have a lower hardness than in the interface, of 382 HV.

The average tensile strength in the welded joint is 138 MPa, which is significantly lower than the other two cases studied.

5. CONCLUSIONS

- Very similar mechanical characteristics are obtained with pearlitic malleable cast iron and Fe-Ni alloy as filler material which is much higher than the yield strength in welding that uses bronze and manganese alloy as filler material. Consequently, regarding the mechanical characteristics, the first two cases (filler materials of pearlitic malleable cast iron and Fe-Ni alloy) should be considered as a better solution.
- In all three cases, the hardness in the interface area is high, which can lead to the fragility of the piece in service. The heat-affected zones have homogeneous hardness, similar to the base metal and the weld zone.
- The study is conclusive in the use of the TIG technique for cold repair welding, which can be presented as an alternative to SMAW welding.
- As for the micrographs studied and correlating them with the values of hardness, tension and elongation. Very homogeneous values are observed in the test carried out with malleable cast iron filler material, a little more disparate in the case of welding with Fe-Ni rod and more discordant values for the case of welding with manganese bronze filler metal.
- In conclusion, this type of welding with filler material and air cooling (weld of cold cast iron), which can be assimilated to repair welding, is valid in the cases and circumstances mentioned in the research, although in general terms it presents results that are not completely satisfactory. As a result, it is advisable to introduce preheating of the pieces before welding and subsequent heat treatments of annealing or standardisation, which will be the object of study in later research.

REFERENCES

Abboud, J.H. (2012). Microstructure and erosion characteristic of nodular cast iron surface modified by tungsten inert gas. *Mater. Design* 35, 677–684. https://doi.org/10.1016/j.matdes.2011.09.029.

Askari-Paykani, M., Shayan, M., Shamanian, M. (2014). Weldability of ferritic ductile cast iron using full factorial design of experiment. *J. Iron Steel Res. Int.* 21 (2), 252–263. https://doi.org/10.1016/S1006-706X(14)60039-X.

Bhatnagar, R.K., Gupta, G. (2016). A Review on Weldability of Cast Iron. *IJSER* 7 (5), 126–131.

Bhatti, A.A., Barsoum, Z., Murakawa, H., Barsoum, I. (2015). Influence of thermo-mechanical material properties of different steel grades on welding residual stresses and angular distortion. *Mater. Design* 65, 878–889. https://doi.org/10.1016/j.matdes.2014.10.019.

Cárcel-Carrasco, F.J., Pérez-Puig, M.A., Pascual-Guillamón, M., Pascual-Martínez, R. (2016). An analysis of the weldability of ductile cast iron using inconel 625 for the root weld and electrodes coated in 97.6% nickel for the filler welds. *Metals* 6 (11), 283. https://doi.org/10.3390/met6110283.

Cárcel-Carrasco, J., Pascual, M., Pérez-Puig, M., Segovia, F. (2017). Comparative study of TIG and SMAW root welding passes on ductile iron cast weldability. *Metalurgija* 56 (1–2), 91–93. http://hdl.handle.net/10251/102690.

Chamim, M., Triyono, Diharjo, K. (2017). Effect of electrode and weld current on the physical and mechanical properties of cast iron welding. *AIP Conf. Proc.* 1788 (1), 030031. https://doi.org/10.1063/1.4968284.

De La Torre, U., Loizaga, A., Lacaze, J., Sertucha, J. (2014). As cast high silicon ductile irons with optimised mechanical properties and remarkable fatigue properties. *Mater. Sci. Tech.* 30 (12), 1425–1431. https://doi.org/10.1179/1743284713Y.0000000483.

Ebrahimnia, M., Ghaini, F.M., Gholizade, S., Salari, M. (2012). Effect of cooling rate and powder characteristics on the soundness of heat affected zone in powder welding of ductile cast iron. *Mater. Design* 33, 551–556. https://doi.org/10.1016/j.matdes.2011.04.063.

El-Banna, E.M. (1999). Effect of preheat on welding of ductile cast iron. *Mater. Lett.* 41 (1), 20–26. https://doi.org/10.1016/S0167-577X(99)00098-1.

Gouveia, R.M., Silva, F.J.G., Paiva, O.C., de Fátima Andrade, M., Pereira, L.A., Moselli, P.C., Papis, K.J.M. (2018). Comparing the structure and mechanical properties of welds on ductile cast iron (700 MPa) under different heat treatment conditions. *Metals* 8 (1), 72. https://doi.org/10.3390/met8010072.

Kumar, R., Kumar, M., Trivedi, V., Bhatnagar, R. (2017). Evaluation of Mechanical and Microstructural Properties of Cast Iron with Effect of Pre Heat and Post Weld Heat Treatment. *Int. J. Mech. Eng.* 4 (5), 1–6. https://doi.org/10.14445/23488360/ijme-v4i5p101.

Marques, E.S.V., Silva, F.J.G., Paiva, O.C., Pereira, A.B. (2019). Improving the mechanical strength of ductile cast iron welded joints using different heat treatments. *Materials* 12 (14), 2263. https://doi.org/10.3390/ma12142263.

Merchant Samir, Y. (2015). A Review of Effect of Welding and Post Weld Heat Treatment on Microstructure and Mechanical Properties of Grade 91 Steel. *IJRET* 4 (3), 574–580. https://doi.org/10.15623/ijret.2015.0403096.

Pascual, M., Ferrer, C., Rayón, E. (2009). Weldability of spheroidal graphite ductile cast iron using Ni / Ni-Fe electrodes. *Rev. Metal.* 45 (5), 334–338. https://doi.org/10.3989/revmetalm.0814.

Sellamuthu, P., Samuel, D.G.H., Dinakaran, D., Premkumar, V.P., Li, Z., Seetharaman, S. (2018). Austempered ductile iron (ADI): Influence of austempering temperature on microstructure, mechanical and wear properties and energy consumption. *Metals* 8 (1), 53. https://doi.org/10.3390/met8010053.

Suárez-Sanabria, A., Fernández-Carrasquilla, J. (2006). Microestructura y propiedades mecánicas de una fundición esferoidal ferrítica en bruto de colada para su uso en piezas de grandes dimensiones. *Rev. Metal.* 42 (1), 18–31. https://doi.org/10.3989/revmetalm.2006.v42.i1.3.

UNE-EN 876 (1996). Ensayos destructivos de uniones soldadas en materiales metálicos. Ensayos de tracción longitudinal sobre el metal de aportación en uniones soldadas por fusión. Normalización Española.

UNE-EN 10002-1 (2002). Materiales metálicos: Ensayos de tracción. Parte 1, Método de ensayo a temperatura ambiente. Asociación Española de Normalización y Certificación.

UNE-EN 1563 (2019). Fundición. Fundición de grafito esferoidal. Normalización Española y Certificación.

Wube Dametew, A. (2015). Experimental investigation on weld ability of cast iron. *Science Discovery* 3 (6), 71-75. https://doi.org/10.11648/j.sd.20150306.15.